

Corrosion Properties of Copper, Nickel, and Titanium in Alkylimidazolium Chloroaluminate Based Ionic Liquids

Qibo Zhang*, Yixin Hua, Zhongren Zhou

Key Laboratory of Ionic Liquids Metallurgy, Faculty of Metallurgical and Energy Engineering, Kunming University of Science and Technology, Kunming 650093, China

*E-mail: qibo Zhang@163.com

Received: 31 March 2013 / Accepted: 19 June 2013 / Published: 1 August 2013

The corrosion properties of copper, nickel, and titanium in both Lewis acidic and basic 1-butyl-3-methyl-imidazolium chloride (BMIC) aluminum chloride (AlCl_3) ionic liquids (ILs) are firstly investigated using potentiodynamic polarization, electrochemical impedance spectroscopy, and scanning electron microscopy. Cu showed a tremendous corrosion in the chloroaluminate ILs. Whereas Ni generally was not attacked in the basic IL, it performed an obvious active-to-passive transition behavior in the acidic IL. Ti was observed to be moderately pitting corroded and active corrosion in the basic and acidic ILs, respectively. Comparing to the traditional chloride-containing aqueous solution, the materials exhibited absolutely distinguished corrosion and passivation behavior in the ILs. In general, the corrosivity of ILs strongly depended on the forms of ions, especially anions in the IL media.

Keywords: Corrosion; Metals; Electrochemical techniques; Electron microscopy (SEM)

1. INTRODUCTION

Ionic liquids (ILs) are organic salts that are liquids at ambient temperature (below 100 °C) and comprised entirely of organic cations and organic/inorganic anions [1]. Because of the unique structure characteristics, ILs have many attractive properties such as intrinsic ionic conductivity, large electrochemical windows, excellent thermal stability, non-volatility, non-flammability, and non-toxicity, which attracted much interest over the past two decades due to their potential applications including electrodeposition, batteries, catalysis, and organic synthesis [2-5]. Although enormous progresses on the application studies of ILs in various fields are made, their industrial applications are practically not implemented, since the chemical environments in ILs are quite different from those in conventional molecular solvents and unpredictable at the current state of knowledge [6], which leads to

insufficiently understand of the chemical processes involved with ILs. The study and characterization of the corrosion behaviors of engineering materials in ILs are highly relevant for many industrial applications, such as the choice of materials for chemical plant components, the construction of thermal storage and exchange devices in chemical reactors, storage, transportation, and operation of ILs. However, the corrosion interaction between materials and ILs, though very critical, has seldom been investigated.

Recently, the corrosion characteristics of several metals and alloys in various ILs have already been studied [7-13]. Titanium resisted corrosion in ambient environments, though it was not passivated in aluminum chloride (AlCl_3)-1-ethyl-3-methylimidazolium chloride (EMIC) IL and became severely corroded under an anodic applied potential [8]. Magnesium and the AZ91 alloys, both characterized by tremendous corrosion rates in aqueous solutions, were practically inert in anhydrous 1-butyl-3-methylimidazolium trifluoromethylsulfonate ($[\text{BMIM}]\text{BF}_4$) [9]. Stainless steel was proved to have excellent resistance to the erosion corrosion in anhydrous systems [10] and localized corrosion was attributed to the presence of Cl^- [11]. Copper has high corrosion susceptibility in both 1-butyl-3-methyl-imidazolium bis-(trifluoro-methanesulfonyl) imide ($[\text{BMIM}][\text{Tf}_2\text{N}]$) [12] and neutral aluminum chloride/1-ethyl-3-methylimidazolium chloride (EMIC- AlCl_3) ILs [7]. AISI 1018 steel, brass and Inconel 600 showed low corrosion current densities in $[\text{BMIM}][\text{Tf}_2\text{N}]$ at room temperature [12]. Furthermore, the presence of water played a crucial role. Aluminum alloys corrosion was found to be negligible in ILs at room temperature. However, addition of water to the ILs was observed to increase their corrosion due to hydrolysis of the anion [13]. In addition, it has been reported that active metals such as lithium and magnesium can react with many of the 2nd and 3rd generation ILs, producing surface protection layers against corrosive environments [14-16], which have also been proposed as methods for the control of the corrosion of metal alloys [17-22].

In this work, some common metal materials, namely copper (Cu), nickel (Ni), and titanium (Ti), are investigated in both Lewis acidic and basic 1-butyl-3-methyl-imidazolium chloride (BMIC) aluminum chloride (AlCl_3) ILs, which are considered as they are extensive application in the electrodeposition of Al [23] and potential useful for directly electrochemical reduction of titanium dioxide [24], respectively. Nevertheless, to our knowledge no information is available about the corrosion characteristics of materials in these acidic and basic chloroaluminate ILs, which have never been explored, except for a preliminary study [25].

2. EXPERIMENTAL SECTION

2.1. Reagents

The BMIC (99.9%) was purchased from Shanghai Chengjie Chemical Co., Ltd. China and used without further treatment. Anhydrous aluminum chloride (99.9%) was used as received. The Lewis acidic and basic BMIC- AlCl_3 RTILs were prepared by the slow addition of a certain weight of AlCl_3 into BMIC at the mole ratio of 2.0:1.0 and 1.0: 2.0 in two flasks, respectively and then heating the

mixture to 80°C with continuously stirring by a magnetic paddle for 24 h to ensure uniformity. The resulting melt was a light yellow liquid at room temperature.

2.2. Electrochemical measurements

Electrochemical impedance spectroscopy (EIS) measurements and potentiodynamic polarization measurements were carried out were accomplished a GAMRY PCI4/300 electrochemical work station. All electrochemical experiments were performed in a conventional three electrodes electrochemical cell at 303K by oil bath thermostat under a purified nitrogen atmosphere. The reference electrode was an Ag wire placed in a fritted glass tube containing BMIC-AlCl₃ RTILs. All potential values determined in this paper were referenced to this electrode. Purity Cu, Ni, Ti disk electrode (Ø 4mm, 99.99%) were used as working electrodes, respectively, and a platinum bar (Ø 1mm, 10mm) directly immersed in the bulk RTILs was used as the counter electrode. All these working electrodes were inserted in a Teflon tube with the exposed surface of 0.1256 cm². Before each experiment the working electrode was polished with 1200 grit silicon carbide paper and 0.5 µm high-purity alumina, rinsed with twice distilled water and finally dried. EIS measurements were performed at open-circuit potentials, over a frequency range of 100 kHz to 50 mHz with a signal amplitude perturbation of 5mV. Potentiodynamic polarization tests were carried out with a sweep rate of 5 mV/s toward an anodic direction. For comparison, the corrosion properties of the same materials in deaerated 3.5 wt.% NaCl aqueous solution were also evaluated. In this case, a platinum sheet and a SCE were used as the counter electrode and the reference electrode, respectively.

After the polarization measurements (both in the BMIC-AlCl₃ IL and NaCl aqueous solution), the electrodes were thoroughly cleaned with anhydrous alcohol and then dried in air. To investigate the material corrosion characteristics, the surface morphologies and chemical compositions of these samples were examined using a scanning electron microscope (SEM, HITACHI S-3400N) and its auxiliary energy-dispersive X-ray spectrometer (EDS), respectively.

3. RESULTS AND DISCUSSION

3.1. Potentiodynamic polarization curves

Polarisation curves for Cu, Ni, Ti in BMIC-AlCl₃ ILs and 3.5 wt% NaCl aqueous solution are presented in Fig. 1, respectively. The polarization parameters (corrosion current densities, i_{corr} and corrosion potentials, E_{corr}) estimated from the polarisation curves, using the Tafel extrapolation method, are tabulated in Table 1. For the NaCl aqueous solution, Ni (dash line in Fig.1 (a)) showed an obvious anodic behavior with the highest corrosion potential (E_{corr} : -0.207 V_{SCE}) and the largest corrosion current of approximately 22.13 µA cm⁻² than those of the other two materials. The anodic current gradually decreased with increasing the electrode potential (above 0.3 V_{SCE}), which could be associated with the formation of the passivation layer (somewhat acted as a barrier). However, the passivation breakdown occurred when the potential became sufficiently high (above 1.4 V_{SCE}).

Similarly, Cu showed rapid anodic dissolution behavior with corrosion current density of approximately $6.815 \mu\text{A cm}^{-2}$ (solid line in Fig.1 (a)).

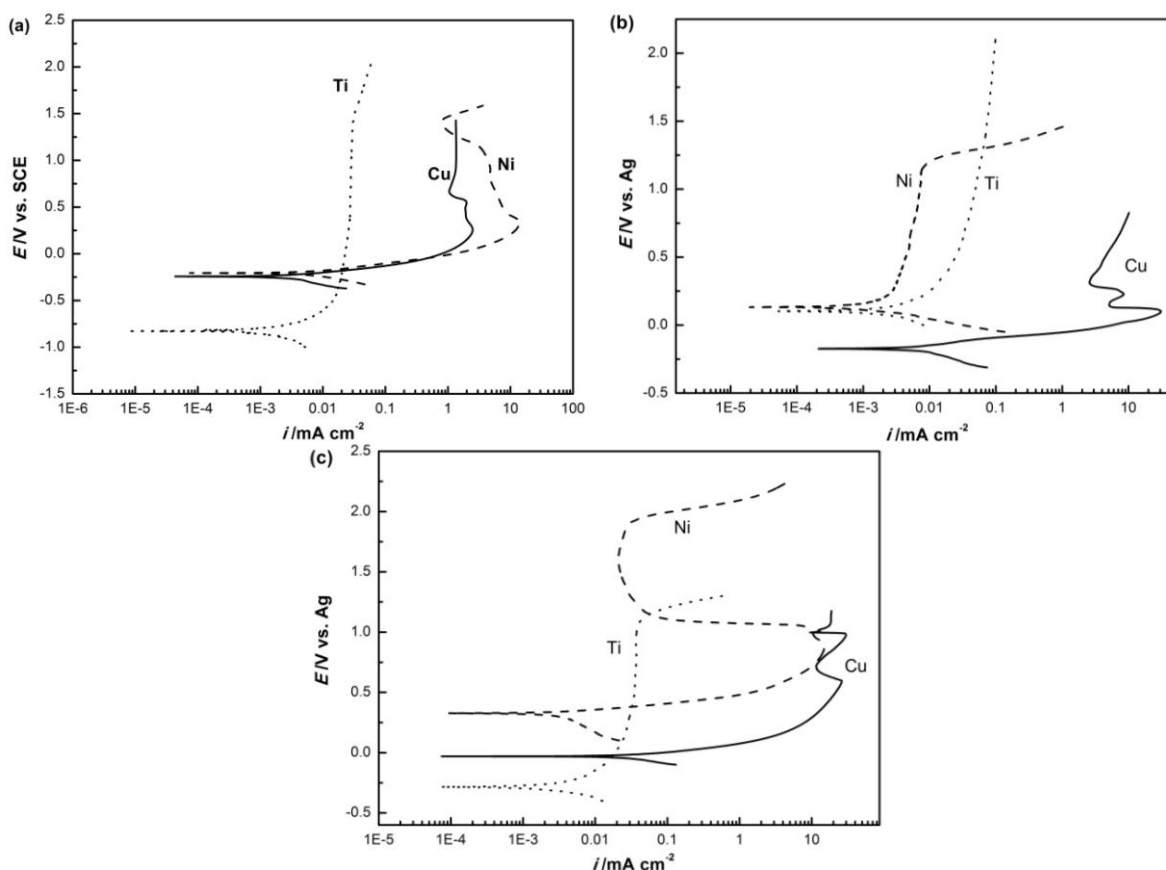


Figure 1. Potentiodynamic polarization curves of Cu (Solid line), Ni (Dash line), and Ti (Dot line) measured in (a) 3.5 wt.% NaCl aqueous solution, (b) basic and (c) acidic BMIC- AlCl_3 ILs.

When the electrode potential was increased to above E_{corr} ($-0.242 \text{ V}_{\text{SCE}}$), the anodic current sharply increased and gradually decreased, which is consistent with results reported in the literature [7]. Ti exhibited a passivation characteristic extending the widest passive region from $\sim -0.49 \text{ V}$ to $1.49 \text{ V}_{\text{SCE}}$ with the smallest minimum passive current density ($\sim 0.02 \text{ mA cm}^{-2}$) (dot line in Fig.1 (a)). The slight slope change at $\sim +1.50 \text{ V}_{\text{SCE}}$ could be attributed to the decomposition of the native Ti oxide formed in air [8].

In the cases of BMIC- AlCl_3 ILs, the corrosion phenomena of these metals are really different, indicating different corrosion mechanism from what was known in traditional aqueous systems. As compared to the case in aqueous solution, Ni showed an obvious active-to-passive transition behavior in the acidic IL (dash line in Fig.1(c)). The active dissolution current density of approximately 9.05 mA cm^{-2} at around $\sim 1.05 \text{ V}_{\text{Ag}}$ dramatically decreased to $< 0.05 \text{ mA cm}^{-2}$ with positively moving of the potential (The active corrosion potential is much lower than passivation potential.). The passive region extended from $\sim 1.17 \text{ V}_{\text{Ag}}$ to a transition potential at $\sim 1.90 \text{ V}_{\text{Ag}}$. Further increasing the potential resulted in an abrupt current at $\sim 2.00 \text{ V}_{\text{Ag}}$, which suggested the decomposition of the IL. Similar to the

literature reported [7] that Ni exhibited a passive transition behavior without the presence of an active region in the neutral EMIC-AlCl₃ IL. For Ni in the basic IL, a single passive transition corrosion phenomenon was obtained (dash line in Fig.1 (b)). When the electrode potential was increased to above E_{corr} ($\sim 0.14 \text{ V}_{\text{Ag}}$), a passive range extending from 0.24 to 1.14 V_{Ag} was observed with the anodic current density as low as 0.01-0.1 mA cm^{-2} . Transpassive behavior was occurred when the applied potential was higher than 1.15 V_{Ag} .

In the acidic IL, Ti was found to be passivated but with narrower passive region appeared in the anodic polarization curve in comparing to the case in aqueous solution. The passivation stage observed was $\sim 1.0 \text{ V}$ (extending from ~ 0.07 to $\sim 1.07 \text{ V}_{\text{Ag}}$) with the measured anodic current density was $\sim 0.03 \text{ mA cm}^{-2}$ (dot line in Fig.1 (c)). As previously described [25], the commercially pure (CP) Ti (99.5%) only exhibited an active dissolution behavior without passive phenomenon in acidic EMIC-AlCl₃ (1:2 in the molar ratio) IL. However, that was evidently different from the high pure Ti (99.99%) in the acidic BMIC-AlCl₃ IL. The explanation should be that the impurities in the CP Ti induced its active dissolution and/or the changes in physicochemical properties such as viscosity, conductivity, ionic activity, etc, arising from the alkyl chain change. In contrast, for Ti in the basic BMIC-AlCl₃ IL (dot line in Fig.1 (b)), no breakdown potential was observed in the studied potential range. The anodic current density was found to gradually and steadily increase when the electrode potential was increased to above $\sim 0.25 \text{ V}_{\text{Ag}}$. However, the current density value was much bigger.

Similar to the traditional aqueous NaCl solution, Cu showed a completely active dissolution phenomenon with corrosion current density of ~ 23.70 and $\sim 16.38 \mu\text{A cm}^{-2}$ in the acidic and basic ILs, respectively (solid line in Fig.1 (b) and (c)). The anodic current sharply increased when the potential was increased to above E_{corr} , and soon reached a steady density ($\sim 18.5 \text{ mA cm}^{-2}$ for the acidic IL and 4.20 mA cm^{-2} for the basic one) with some current fluctuations, which may be ascribed to the potential-derived microstructure change of the surface.

3.2. Impedance spectra

Corrosion susceptibility of these metal materials was evaluated by means of EIS under an open-circuit condition. Fig. 2 shows the Nyquist plots of Cu, Ni, and Ti measured in the chloroaluminate ILs and NaCl aqueous solution, respectively. As can be seen, each impedance spectra obtained yield depressed semicircles, which is essentially characterized by a single time constant equivalent circuit. The semicircular depression in the Nyquist diagram was attributed to the heterogeneity of the surface [27]. R_p , is the polarization resistance of the metal/electrolyte interface at which corrosion occurs, which can be regarded as an indicator of the extent of corrosion acceptability (A higher R_p indicates a lower corrosion susceptibility or a greater stability of the material/electrolyte conjunction). The R_p value can be obtained from a nonlinear least-squares fitting of the impedance semicircle. The fitting results are summarized in Table 2.

As shown in Fig 2, the diameter of the semi-circle of the capacitive loop of the Cu in ILs was much smaller than that of the NaCl traditional aqueous solution. In other words, Cu in aqueous solution presented a higher R_p than that measured in ILs ($12.47 \text{ k}\Omega \text{ cm}^2$ in NaCl, 1.796 and 5.478 $\text{k}\Omega$

cm^2 in the acidic and basic ILs, respectively). In the electrochemical reaction, R_p , reflects the corrosion rate of a material in a corrosive media.

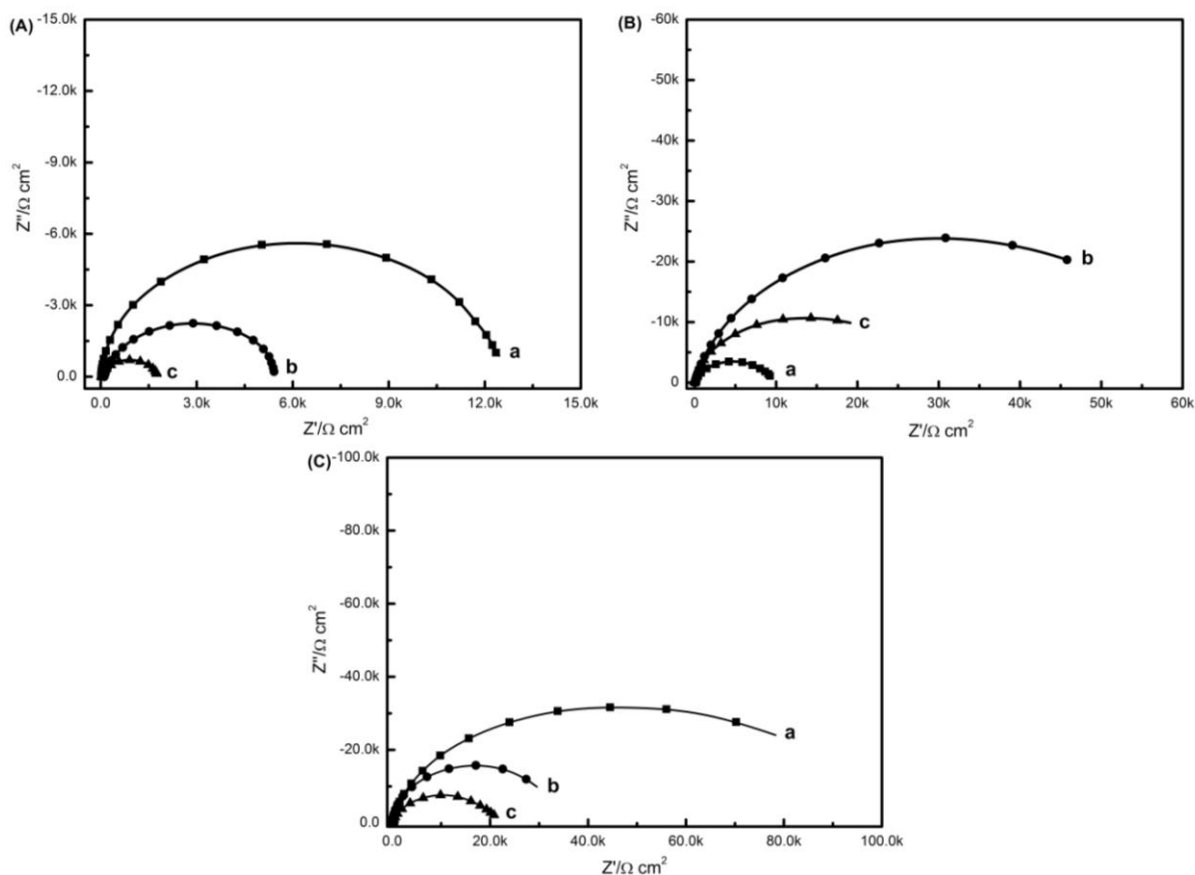


Figure 2. Nyquist plots for (A) Cu, (B) Ni, (C) Ti recorded in 3.5 wt.% NaCl aqueous solution (curves a), basic (curves b), and acidic (curves c) BMIC- AlCl_3 ILs. The samples are measured at the respective open-circuit potential.

The larger the R_p , the slower the corrosion rate. Therefore, high R_p of Cu suggested its high acceptability to the former corrosive environment. Similar observation was obtained in the case of Ti. Ti showed a clearly lower R_p value of 34.53 and 22.13 $\text{k}\Omega \text{cm}^2$ in the acidic and basic ILs, respectively, as compared to that measured in the chloride-containing aqueous solution where the R_p obtained was 92.37 $\text{k}\Omega \text{cm}^2$, revealing its poor corrosion resistance in the chloroaluminate ILs. One explanation is that the metal oxide layers/passive films dissolved and barely re-formed in the low-oxygen and high-ion-containing ILs media, resulting in the rapid corrosion of metal. Additionally, the different corrosion susceptibility performance of the same material between acidic and basic ILs may be explained by the different chemical nature of the constituent ions in ILs and the corrosion character of the material itself. As known that, Cl^- and BMIM^+ are the main constituent species in the basic BMIC- AlCl_3 IL, while for the acidic case, Al_2Cl_7^- and BMIM^+ are the main constituent species [28]. The attack of Al_2Cl_7^- in acidic IL on Ti seems much weaker than that of Cl^- in basic IL does. But in the case of Cu, the effect is actually just the opposite.

Unexpectedly, Ni, which was most easily corroded in NaCl aqueous solution ($R_p = 10.05 \text{ k}\Omega \text{ cm}^2$), exhibited the best stability in the Lewis acidic ($24.79 \text{ k}\Omega \text{ cm}^2$) and basic ($60.16 \text{ k}\Omega \text{ cm}^2$) ILs. However, the excellent corrosion resistance performance of Ni in ILs has not yet been clear. It is suspected that some steady adsorbed species formed at the Ni/electrolyte interface hindered it from being attacked, that should be further verification. All these experimental results are in agreement with that obtained from potentiodynamic polarization measurements and point out that the corrosion phenomena in the two systems are really divergent.

3.3. Surface corrosion characteristics

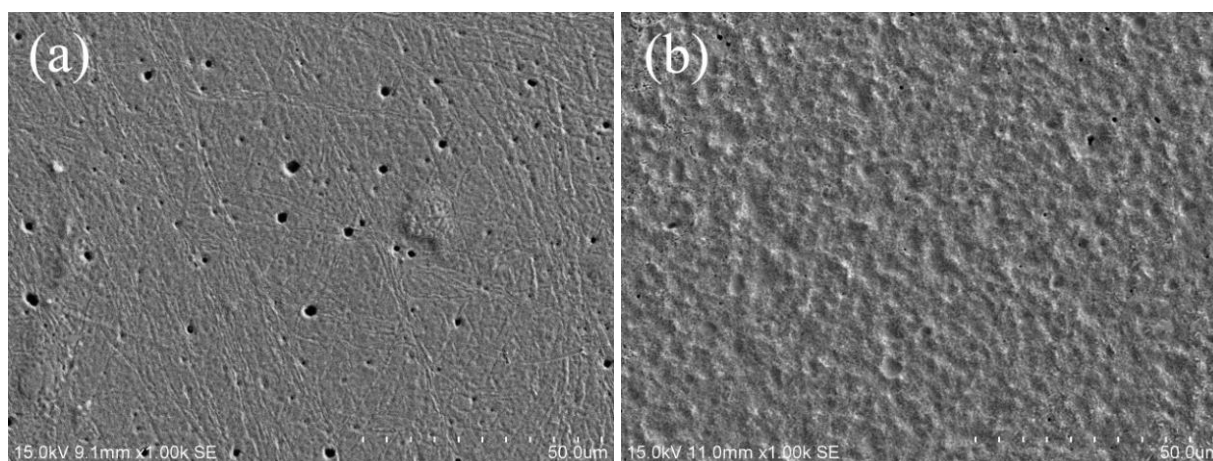


Figure 3. SEM micrographs of Cu polarized at (a) $0.2 \text{ V}_{\text{Ag}}$ and (b) $0.8 \text{ V}_{\text{Ag}}$ for 30 min in basic and acidic BMIC- AlCl_3 ILs, respectively.

To explore the surface corrosion characteristics and the passivation behavior of these metals in the Lewis acidic and basic BMIC- AlCl_3 ILs, the samples after anodic potentiodynamic polarization tests were examined using SEM and EDS. Unfortunately, the surface formed passivation film may be soluble in the alcohol washing during the post cleaning process or too thin to be detected using EDS. In all cases in this study, only metal and trace O elements can be found on these metal electrodes, no other elements like Al and Cl existed. Further surface analyses using X-ray photoelectron spectroscopy (XPS) to detect the chemical compositions of the passive layer film are in progress, however, the extremely easy oxidation of the outmost film upon exposure of the sample in air is a big challenge.

Fig. 3 showed the corrosion surface morphologies of Cu. Several corrosion pits with diameters about $5 \mu\text{m}$ appeared on the surface of Cu polarized at $0.2 \text{ V}_{\text{Ag}}$ for 30 min in basic IL (Fig. 3(a)), revealing that severe corrosion occurred on Cu surface. Similarly, Cu was observed severely corroded in acidic IL after being held at $0.8 \text{ V}_{\text{Ag}}$, as shown in Fig. 3(b). However, the morphologies provided visual distinct characteristics in the two ILs. The latter sample was evidently dissolved, leaving behind a rough and massif-like surface without corrosion pits. This result should be attributed to the difference in the forms of ions, especially anions in the two ILs as mentioned above. Chemistry of the anions seems to play greater role in altering the corrosion properties of ILs.

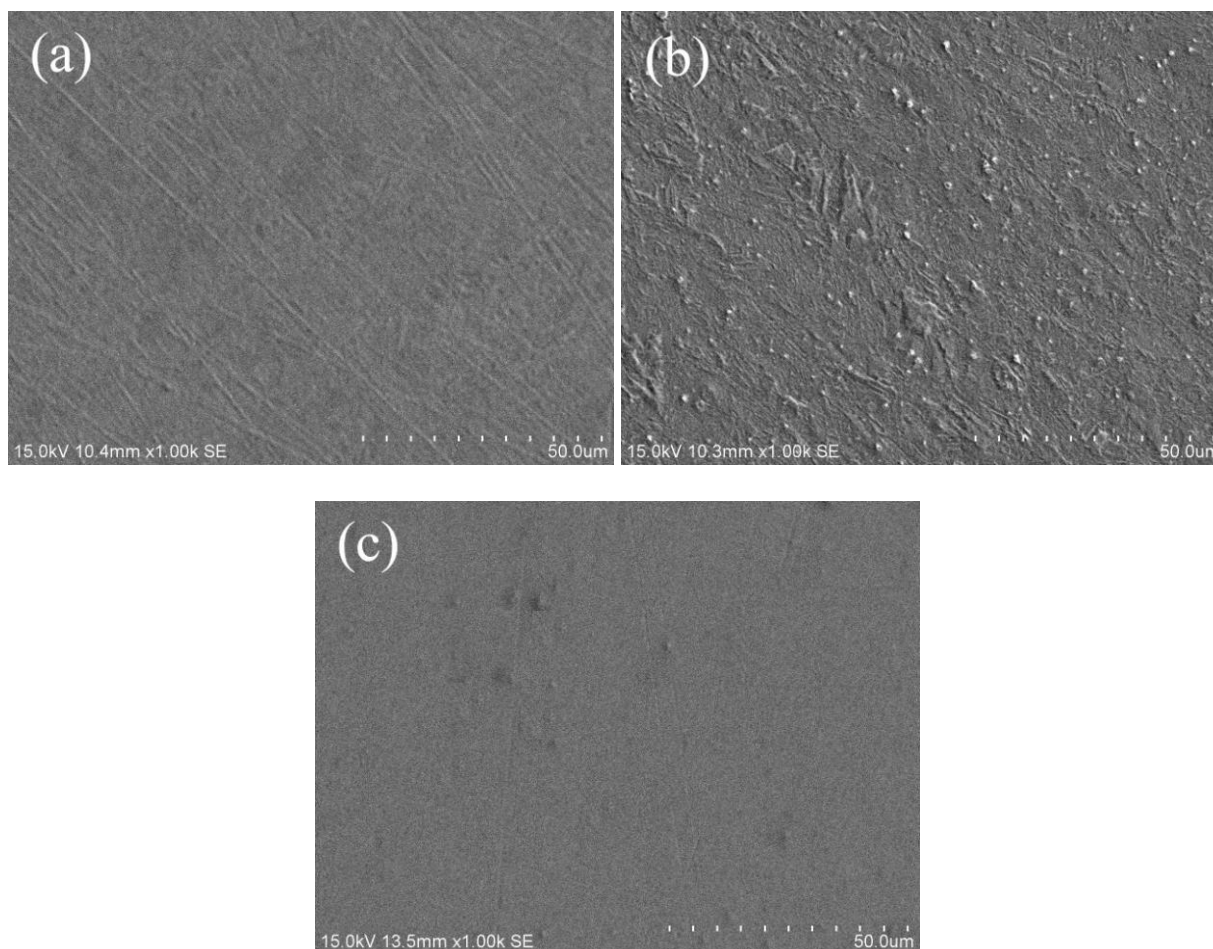


Figure 4. SEM micrographs of Ni after being held at (a) 1.0 V_{Ag} for 30 min in basic BMIC- $AlCl_3$ IL and polarized at (b) 0.8 V_{Ag} , and (c) 1.5 V_{Ag} for 30 min in acidic BMIC- $AlCl_3$ IL, respectively.

Fig.4(a) showed the SEM micrograph of Ni after being held at 1.0 V_{Ag} for 30 min in basic IL. No evidence of localized corrosion occurred for Ni. The original grinding scratches observed on the corrosion surface without changing after the potentiostatic test indicated that the Ni exhibited excellent pitting resistance. This is different from what is typically observed in the Cl^- containing aqueous corrosive environments, where Ni is severely corroded [26], which should be attributed to the difference in the activity of Cl^- and the surface status of Ni in the two different environments. In the acidic IL, serious general corrosion on Ni surface was observed at the active potential (Fig.4(b)). However, it became inert when the applied potential was sufficiently high at 1.5 V_{Ag} (with in the passive region) (Fig.4(c)). As compared to the cases in aqueous solution and basic IL, Ni showed an obvious active-to-passive transition property in the acidic IL. This result was quite in agreement with the above potentiodynamic polarization curve measurement (dash line in Fig.1(c)).

Interestingly, in comparing to its excellent corrosion resistance in traditional chloride-containing aqueous solution, localized pitting corrosion was observed after Ti being held at 1.0 V_{Ag} (the apparent passive region potential) for 30 min in basic IL, as shown in Fig.5(a), indicating the poor pitting corrosion resistance of Ti in this IL media. For the case of acidic IL, Ti exhibited a complete integrity in the IL by polarizing at 0.8 V_{Ag} (with in the passive region) for 30 min (Fig.5(b)). As

expected, when the applied potential was beyond the transpassive potential, Ti was severely corroded in the IL (Fig.5(c)). The surface was rough and covered with a large number of corrosion irregular button-like grooves.

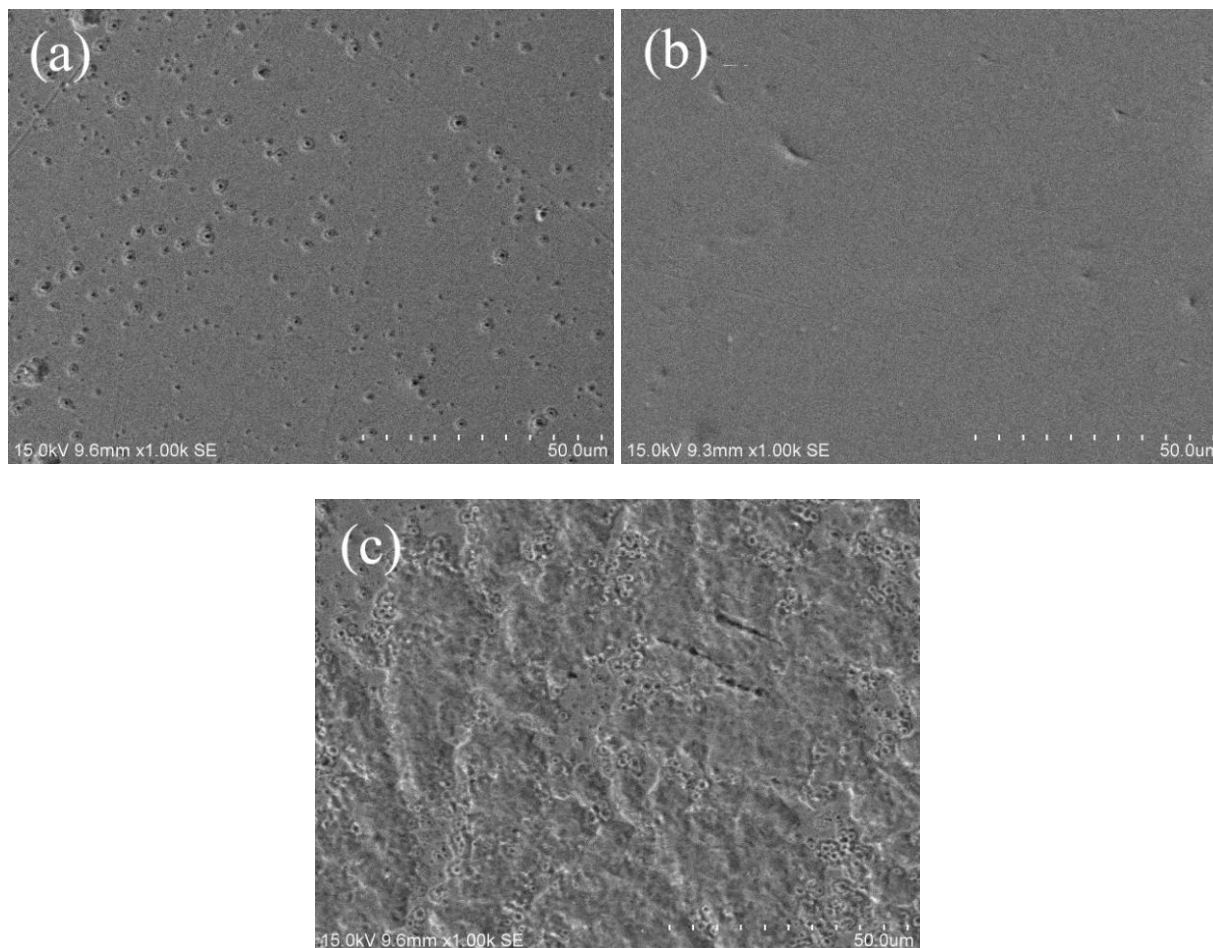


Figure 5. SEM micrographs of Ti after being held at (a) 1.0 V_{Ag} for 30 min in basic BMIC-AlCl₃ IL and polarized at (b) 0.8 V_{Ag}, and (c) 1.5 V_{Ag} for 30 min in acidic BMIC-AlCl₃ IL, respectively.

4. CONCLUSIONS

The corrosion behaviors of copper, nickel, and titanium in both Lewis acidic and basic BMIC-AlCl₃ ILs are found to be quite different from those known in traditional chloride-containing aqueous solution. Whereas Ti was severely corroded in the IL media, it exhibited inert nature in the traditional aqueous solution. Ni exhibited the highest corrosion resistance with a wide passive range and low passive current density in both acidic and basic ILs. This material can, therefore, be recommended for the ideal conductive material in the BMIC- AlCl₃ ILs. However, the abnormal corrosion characteristics of Ni in the acidic IL, where active corrosion potential was observed to be much lower than passivation potential, should be attracted attention as its severe corrosion damage occurred at a slightly anodic polarization condition. Cu showed the lowest corrosion resistance in the IL media, which is

much more profound than that of in aqueous NaCl solution. For this reason, the use of Cu as the substrate material for Al electrodeposition from acidic BMIC- AlCl₃ IL should be essentially avoided and different material choices have to be made. These findings indicate that the corrosion characteristics of materials in ILs are dissimilar to the cases in the traditional aqueous systems and their selection for engineering used in ILs involved chemical processes is a very important issue.

Depending on the forms of ions, especially anions in the IL media, the material corrosion behaviors in ILs and the corrosivity of the ILs were really distinct. Ti underwent severe corrosion in the acidic IL, while moderately localized pitting corrosion phenomena occurred in the basic IL. Similar, severe corrosion with and without visual corrosion pits was clearly observed for Cu in the basic and acidic ILs, respectively. Ni that generally was not attacked in the basic IL, exhibited an active-to-passive transition behavior in the acidic IL. Since the corrosion mechanism and its relation to chemical nature of the constituent ions in ILs are still far from being fully understood, further investigations with respect to these issues should be studied in more detail.

ACKNOWLEDGEMENTS

The authors gratefully acknowledge the financial support of the National Natural Science Foundation of China (51204080, 51274108 and 21263007), Natural Science Foundation of Yunnan Province (2011FA009), and Application Foundation Research of Yunnan Province (2011FZ020).

References

1. K. Seddon, *Nat. Mater*, 2 (2003) 363.
2. A. Balducci, U. Bardi, S. Caporali, M. Mastragostino, F. Soavi, *Electrochem. Commun*, 6 (2004) 566.
3. F. Enders, S. Z. E. Abedin, *Phys. Chem. Chem. Phys*, 8 (2006) 2101.
4. M. J. Earle, J. Esperanca, M. A. Gilea, J. N. C. Lopes, L. P. N. Rebelo, J. W. Magee, K. R. Seddon, J. A. Widegren, *Nature*, 439 (2006) 831.
5. J. K. Chang, M. T. Lee, W. T. Tsai, M. J. Deng, I. W. Sun, *Chem. Mater*, 21 (2009) 2688.
6. G. C. Tian, J. Li, Y. X. Hua, *Trans. Nonferrous. Met. Soc. China*, 20 (2010) 513.
7. P. C. Lin, I. W. Sun, J. K. Chang, C. J. Su, J. C. Lin, *Corros. Sci*, 53 (2011) 4318.
8. C. H. Tseng, J. K. Chang, J. R. Chen, W. T. Tsai, M. J. Deng, I. W. Sun, *Electrochem. Commun*, 12 (2010) 1091.
9. A. Shkurankov, S. Z. E. Abedin, F. Endres, *Aust. J. Chem*, 60 (2007) 35.
10. M. Uerdingen, C. Treber, M. Balsler, G. Schmitt, C. Werner, *Green. Chem*, 7 (2005) 321.
11. R. G. Reddy, Z. J. Zhang, M. F. Arenas, D. M. Blake, *High. Temp. Mater. Processes*, 22 (2003) 87.
12. I. Perissi, U. Bardi, S. Caporali, A. Lavacchi, *Corros. Sci*, 48 (2006) 2349.
13. M. D. Bermudez, A. E. Jimenez, G. Marti'nez-Nicola's, *Appl. Surf. Sci*, 253 (2007) 7295.
14. P. C. Howlett, N. Brack, A. F. Hollenkamp, M. Forsyth, D. R. MacFarlane, *J. Electrochem. Soc*, 153 (2006) A595.
15. S. Caporali, F. Ghezzi, A. Giorgetti, A. Lavacchi, A. Tolstogousov, U. Bardi, *Adv. Eng. Mater*, 9 (2007) 185.
16. P. C. Howlett, T. Khoo, G. Mooketsi, J. Efthimiadis, D. R. MacFarlane, M. Forsyth, *Electrochim. Acta*, 55 (2010) 2377.
17. A.B. Tolstoguzov, U. Bardi and S. P. Chenakin, *Bull. Russ. Acad. Sci. Phys*, 72 (2008) 605.
18. N. Birbilis, P. C. Howlett, D. R. MacFarlane, M. Forsyth, *Surf. Coat. Technol*, 201 (2007) 4496.

19. P. C. Howlett, W. Neil, T. Khoo, J. Sun, M. Forsyth, D. R. MacFarlane, *Isr. J. Chem*, 48 (2008) 313.
20. U. Bardi, S.P. Chenakim, A. Lavacchi, C. Pagura, A. Tolstogousov, *Appl. Surf. Sci*, 252 (2006) 7373.
21. J. L. Goldman, A.B. McEwen, *Electrochem. Solid-State. Lett*, 2 (1999) 501.
22. S. Z. E. Abedin, U. Welz-Biermann, F. Endres, *Electrochem. Commun*, 7 (2005) 941.
23. M. Zhang, V. Kamavaram, R. G. Reddy, *Miner. Metall. Proc*, 23 (2006) 177.
24. X. Y. Zhang, Y. X. Hua, C. Y. Xu, Q. B. Zhang, X. B. Cong, N. Xu, *Electrochim. Acta*, 56 (2011) 8530.
25. J. R. Chen, W. T. Tsai, I. W. Sun, *J. Electrochem. Soc*, 159 (2012) C298.
26. L. Liu, Y. Li, F. H. Wang, *Electrochim. Acta*, 53 (2007) 7193.
27. R. S. Goncalves, D. S. Azambuja, A. M. S. Lucho, *Corros. Sci*, 44 (2002) 467.
28. F. Endres, D. MacFarlane, A. Abbott, *Electrodeposition from Ionic Liquids*, Weinheim, Wiley-VCH, 2008, Ch.2.